Supporting Information

Siu et al. 10.1073/pnas.0813113106

SI Materials and Methods

$CdCl_2$-Induced BTB Disruption In Vivo. Adult rats, ≈300 g b.w., were treated with $CdCl_2$ dissolved in saline (20 mg/ml) at 3 mg/kg b.w., i.p., as described previously (1). At selected time points (n = 6 rats for each time point), rats were killed by CO_2 asphyxiation. Testes were immediately removed, frozen in liquid nitrogen, and stored at −80 °C until use, or processed for IHC. Testes lysates were prepared in IP lysis buffer [50 mM Tris, 0.15 M NaCl, 1% Nonidet P-40 (vol/vol), 1 mM EGTA, 2 mM N-ethylmaleimide, 10% glycerol (vol/vol), and 1 mM PMSF, supplemented with phosphatase inhibitor cocktails 1 and 2 and protease inhibitor mixture (15 μL/mL of each inhibitor mixture; Sigma-Aldrich), pH 7.4, at 22 °C].

Immunoblot Analysis, Co-IP and Assessment of the Occludin Phosphorylation Status by Anti-phospho-Tyr, -Ser, and -Thr Antibodies. Co-IP and immunoblot analysis were performed as previously described (2). Co-IP was performed by using 700 μg or 250 μg of protein from lysates of testes or Sertoli cells, respectively. To assess occludin phosphorylation status, anti-occludin antibody was used as the precipitating antibody to first isolate occludin from Sertoli cell lysates by immunoprecipitation to be followed by its subsequent analysis by immunoblotting using different anti-phospho-Tyr, -Ser, and -Thr antibodies using an approach described earlier (3, 4). Briefly, occludin isolated from these lysates by immunoprecipitation was confirmed by immunoblotting using an anti-occludin antibody in pilot experiments. Thereafter, these samples were resolved by SDS-PAGE, and immunoblot analysis was carried out using antibodies specific against phospho-Tyr, -Ser, or -Thr (see Table S1). These blots were stripped and re-probed with an anti-occludin antibody to verify that the levels of occludin between Sertoli cells transfected with the FAK siRNAi duplexes and nontargeting control siRNA duplexes were uniform. The protein band on the blot with the same electrophoretic mobility as of occludin (65 kDa) was thus identified and scanned for densitometric analysis. As such, any changes in Tyr, Ser, or Thr phosphorylation seen were the result of putative changes in the occludin phosphorylation status. The same samples used for Co-IP to assess occludin−ZO-1 interaction and for occludin phosphorylation status analysis were also resolved by SDS-PAGE and immunoblotting to confirm that FAK knockdown indeed had occurred, and no changes in the steady-state protein levels of occludin and ZO-1 were detected. The source and working dilution of antibodies used for different Co-IP and immunoblotting experiments can be found in Table S1.

IHC and Dual-Labeled Immunofluorescent Analysis. IHC and fluorescent microscopy were performed essentially as described previously (2). Briefly, cross-sections of testes or Sertoli cells at each time point including treated testes and/or cells vs. controls were processed in an experimental session to minimize interexperimental variations. All images were captured using an Olympus BX61 fluorescent microscope with a built-in Olympus DP71 12.5 MPa digital camera and acquired as TIFF images using the Olympus MicroSuite Five software package (version 1224) (Olympus Soft Imaging Solutions). Images obtained from dual-labeled immunofluorescent microscopy were merged and analyzed for protein colocalization using Adobe PhotoShop in Creative Suite Design Premium (version 3.0; Adobe Systems). Micrographs reported herein are results of representative sets of at least 3 independent experiments.

Assessment of Sertoli Cell TJ Permeability Barrier by Transepithelial Electrical Resistance (TER) Measurement. Sertoli cells at 1.2 × 10^6 cells/cm^2 were plated on Matrigel-coated Millipore Millicell-HA bicameral units (≈0.6-cm^2 surface area, 0.45-μm pore size containing 0.5-ml F12/DMEM, designated the apical chamber or apical compartment), wherein units were placed in 24-well dishes, with each well containing 0.5-ml F12/DMEM, designated the basal chamber or basal compartment. TER across the cell epithelium was monitored to assess the TJ permeability barrier as described previously (5). It was noted that functional BTB was established as manifested by the presence of ultrastructures of TJ, basal ES, and desmosome-like junction that mimicked the BTB in vivo (6), and the TER reached its plateau by day 3. Cells were then transfected with 200 nM of FAK-specific siRNA duplexes vs. nontargeting control duplexes using 7 μL of TransIT-TKO transfection reagent (Mirus Bio) in F12/DMEM in the bicameral unit in a final reaction volume of 0.5-ml, and TER across the Sertoli cell epithelium was measured every 12 h. Transfection mixture was replaced 24 h thereafter with F12/DMEM, and cells were cultured for an additional 3 days without treatment or were treated with either vehicle (0.9% NaCl) or $CdCl_2$ (0.1 μM) for 8 h. Treated cells were washed twice with F12/DMEM to remove $CdCl_2$. In selected experiments, after treatment with $CdCl_2$, cells were cultured in the absence or presence of testosterone (2×10^{-7} M) to assess the effects of androgen to "reseal" the disrupted TJ barrier. Furthermore, parallel experiments were performed to validate the efficacy of FAK knockdown by immunoblotting using cells cultured on 24-well plates and transfected under the same conditions described above and harvested 24 h after transfection.

Primary Sertoli Cell Cultures. Sertoli cells were isolated from 20-day-old rat testes (6) and plated on Matrigel (BD Biosciences; diluted in F12/DMEM 1:7)-coated dishes at 0.4–1.2 × 10^6 cells/cm^2. Approximately 48 h thereafter, these cultures were subjected to a hypotonic treatment to lyse residual germ cells (7). As such, these cultures had a Sertoli cell purity of >98%, with negligible germ and Leydig cell contamination. By approximately 2 to 3 days, these cells form an intact epithelium with the functional TJ permeabilty barrier when monitored by quantifying TER across the cell epithelium (5). Furthermore, ultrastructures of TJ, basal ES, and desmosome-like junction were also detected by 24–48 h using electron microscopy (6), mimicking the BTB in vivo.

General Methods. Protein concentration was performed by using BioRad Dc Protein Assay Kits with BSA as a standard and a BioRad Model 680 microplate reader. For in vivo experiments, 6 rats were used per time point, and data reported herein are representative of at least 3 different experiments excluding pilot experiments. All in vitro experiments using Sertoli cell cultures, such as studies by RNAi, were repeated at least 4 to 5 times with duplicate or triplicate dishes or bicameral units using different batches of Sertoli cells.

1. Wong CH, Mruk DD, Lui WY, Cheng CY (2004) Regulation of blood-testis barrier dynamics: An in vivo study. *J Cell Sci* 117:783–798.

2. Wong EWP, Mruk DD, Lee WM, Cheng CY (2008) Par3/Par6 polarity complex coordinates apical ectoplasmic specialization and blood-testis barrier restructuring during spermatogenesis. *Proc Natl Acad Sci USA* 105:9657–9662.
3. Lui WY, Lee WM, Cheng CY (2003) Sertoli-germ cell adherens junction dynamics in the testis are regulated by RhoB GTPase via the ROCK/LIMK signaling pathway. *Biol Reprod* 68:2189–2206.
4. Xia W, Cheng CY (2005) TGF-β3 regulates anchoring junction dynamics in the seminiferous epithelium of the rat testis via the Ras/ERK signaling pathway: An in vivo study. *Dev Biol* 280:321–343.
5. Yan HHY, Mruk DD, Wong EWP, Lee WM, Cheng CY (2008) An autocrine axis in the testis that coordinates spermiation and blood-testis barrier restructuring during spermatogenesis. *Proc Natl Acad Sci USA* 105:8950–8955.
6. Siu MKY, Wong CH, Lee WM, Cheng CY (2005) Sertoli-germ cell anchoring junction dynamics in the testis are regulated by an interplay of lipid and protein kinases. *J Biol Chem* 280:25029–25047.
7. Galdieri M, Ziparo E, Palombi F, Russo M, Stefanini M (1981) Pure Sertoli cell cultures: A new model for the study of somatic-germ cell interactions. *J Androl* 2:249–254.

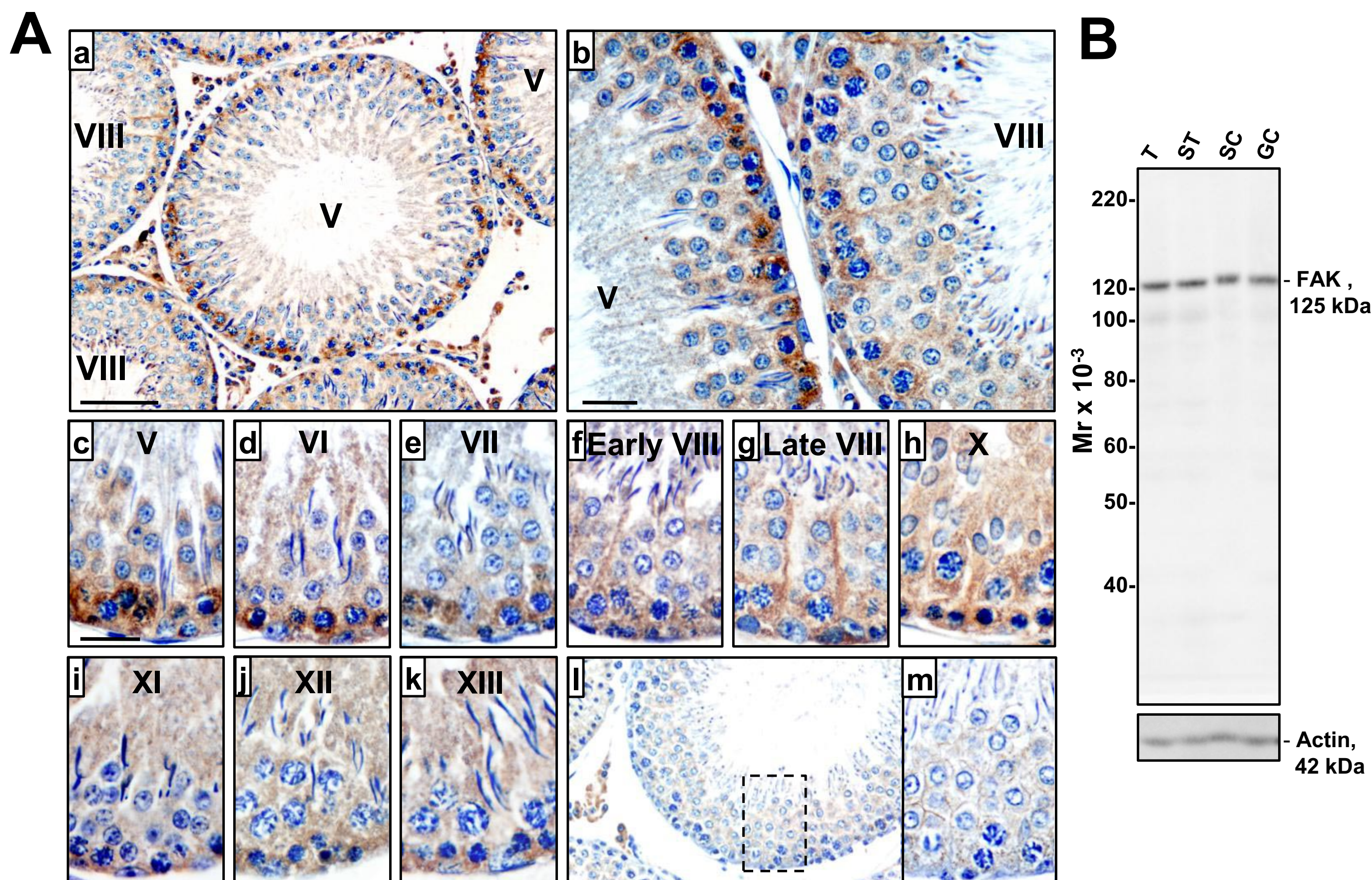

Fig. S1. Stage-specific expression of FAK at the BTB in the seminiferous epithelium of adult rat testes. (*A*) Immunohistochemistry was performed in paraffin sections of adult rat testes by using a specific anti-FAK antibody (see Table S1). (*a* and *b*) Micrographs showing the localization of FAK, which appears as reddish-brown precipitates in the seminiferous epithelium near the basal compartment, consistent with its localization at the BTB in different staged tubules. It is also apparent that the FAK staining is considerably higher at the BTB in stage-V tubules vs. stage-VIII tubules. (*c*–*k*) High-magnification micrographs illustrating the stage-specific expression of FAK in rat testes, with lowest levels at stage VIII–IX (*f* and *g*), at the time BTB restructures [Russell LD (1977) Movement of spermatocytes from the basal to the adluminal compartment of the rat testis. *Am J Anat* 148:313–328] to allow the passage of primary leptotene spermatocytes from the basal to the adluminal compartment. (*l*) Negative control using rabbit IgG instead of anti-FAK antibody for staining; the boxed area is magnified in *m*, illustrating that the FAK staining shown in *a*–*k* is specific. (Scale bars, 100 μm in *a*, which also applies to *l*; 30 μm in *b*; 30 μm in *c*, which also applies to *d*–*k* and *m*.) (*B*) Immunoblot analysis shows the specificity of the antibody used for IHC with lysates of adult rat testis (T), seminiferous tubules (ST), Sertoli cells (SC), and germ cells (GC) (≈50 μg protein/lane).

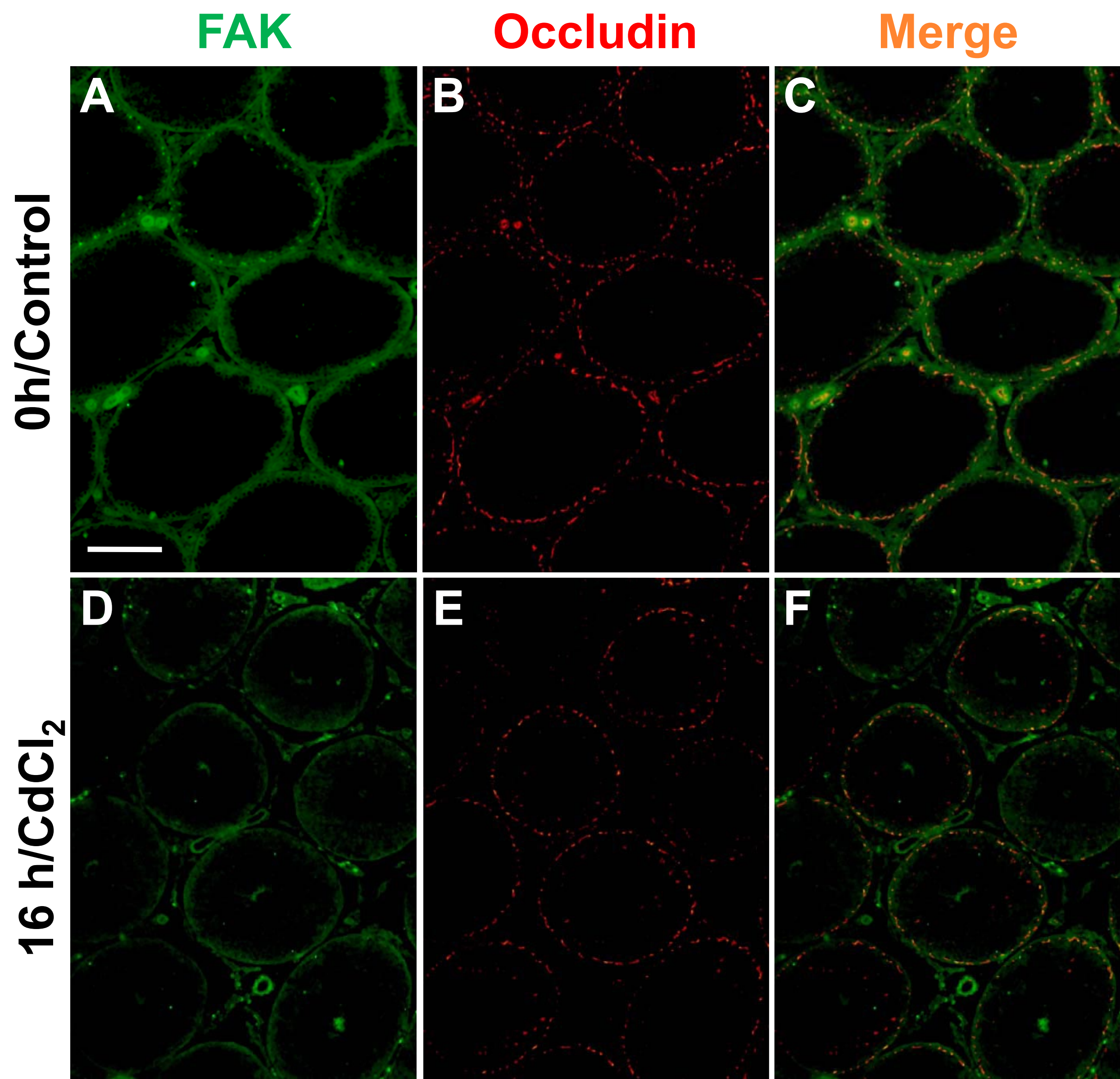

Fig. S2. Colocalization of FAK and occludin in adult rat testes. Frozen sections of testes from normal (control, 0 h; *A–C*) and $CdCl_2$-treated (3 mg/kg b.w., i.p.; 16 h; *D–F*) rats were processed for dual-labeled immunofluorescent analysis with specific anti-FAK and anti-occludin antibodies. Low-magnification micrographs showing staining for FAK (green) and occludin (red) in the seminiferous epithelium near the basement membrane, which is consistent with their localization at the BTB, in both control and $CdCl_2$-treated rats. Colocalization of these proteins is shown in merged images (*C* and *F*). Although the staining for both proteins was reduced at 16 h after $CdCl_2$ treatment (*A* vs. *D*; *B* vs. *E*), FAK and occludin colocalization remained clearly visible (*C* vs. *F*). (Scale bar, 300 μm in *A*, which applies to *B–F*.)

Table S1. Specifications of primary antibodies used for different experiments*

Vendor	Antibody	Catalog no.	Lot no.	Working dilution or amount
Santa Cruz Biotechnology	Mouse monoclonal anti-c-Src	sc-8056	K0507	IB,1:300
	Goat polyclonal anti-actin	sc-1616	H0808	IB, 1:200
	Rabbit polyclonal anti-β1-integrin	sc-8978	H2107	IB, 1:300
	Rabbit polyclonal anti-β-catenin	sc-7199	L0507	IB, 1:200
	Rabbit polyclonal anti-N-cadherin	sc-7939	J2105	IB, 1:200
Upstate/Millipore	Mouse monoclonal anti-FAK	05-537	DAM1432863	IF, 1:100
	Rabbit polyclonal anti-FAK	06-543	31701	IB, 1:1,000 IHC, 1:100 Co-IP, 2 μg
	Rabbit polyclonal anti-p-FAK-Tyr^{576}	07-157	DAM1394797	IB, 1:1,000
	Mouse monoclonal anti-p-Src-Tyr^{416}	05-677	0080S0607	IB, 1:1,000
Abcam	Rabbit monoclonal anti-p-Src-Tyr^{529}	ab32078	391095	IB, 1:7,500
Biosource/Invitrogen	Rabbit monoclonal anti-p-FAK-Tyr^{397}	44-625G	319018A	IB, 1:1,000
Zymed/Invitrogen	Rabbit polyclonal anti-occludin	71-1500	366532A and 455976A	IB, 1:250 IF, 1:50 Co-IP, 2 μg
	Rabbit polyclonal anti-ZO-1	61-7300	389452A	IB, 1:300 IF, 1:50 Co-IP, 2 μg
	Rabbit polyclonal anti-JAM-A	36-1700	370923A	IB, 1:300 IF, 1:50
	Rabbit polyclonal anti-claudin-11	36-4500	387613A	IB, 1:250
	Rabbit polyclonal anti-phosphoserine	61-8100	40487618	IB, 1:500
	Rabbit polyclonal anti-phosphothreonine	71-8200	10665586	IB, 1:500
	Rabbit polyclonal anti-phosphotyrosine	61-5800	40286685	IB, 1:500
Cell Signaling	Rabbit polyclonal anti-p38 MAPK	9212	8	IB, 1:1,000
	Rabbit polyclonal anti-p-p38 MAPK	9211	16	IB, 1:1,000

IB, immunoblotting; IF, immunofluorescent microscopy.

*All primary antibodies used in IB and IF were diluted in BSA (0.1% in PBS–Tris and 1% in PBS, respectively), and for IHC, 10% normal goat serum in PBS; PBS, 10 mM sodium phosphate and 0.15 M NaCl, pH 7.4, at 22°C; PBS-Tris, PBS with 10 mM Tris, pH 7.4, at 22°C.